



SMAR 2024 – 7th International Conference on Smart Monitoring, Assessment and Rehabilitation of Civil Structures

Assessment of the structural integrity of glulam using modal analysis and finite element updating

Ramon Sancibrian^{a*}, Ignacio Lombillo^a, Rebeca Sanchez^a, Alfonso Lozano^b

^aDepartment of Structural and Mechanical Engineering, University of Cantabria, Avda. de los Castros s/n, Santander 39005 Spain

^bDepartment of Construction and Manufacturing Engineering, C/ Pedro Puig Adam Modulo 7, Gijon 33203 Spain

Abstract

The increasing adoption of glued laminated timber (Glulam) as an environmentally conscious material in construction has been driven by its excellent structural properties and lower carbon footprint compared to other conventional materials. However, its organic nature underscores the need to ensure the long-term integrity of these glulam structures. This paper proposes a novel approach to non-destructive testing (NDT) through the combined application of modal analysis and updated finite element modelling. These advanced techniques allow a more accurate and detailed assessment of the structural condition of glulam. Modal analysis identifies changes in natural frequencies and vibration modes caused by potential material degradation, providing valuable structural health information without compromising the integrity of the material. To achieve this objective, the paper proposes to compare the real values measured in the modal analysis with those obtained from the numerical model by formulating an objective function that measures the error between the two. The differences between the two models are reduced using techniques based on Particle Swarm Optimization (PSO). The work presents a specific formulation aimed at achieving greater efficiency in the search for defects in this material. The results of the proposed method are verified by laboratory tests. For this purpose, glulam samples with different defects were tested and their identification was verified by updating the finite element models, demonstrating the ability and accuracy of the method to identify areas where the structural stiffness has decreased due to deterioration.

© 2024 The Authors. Published by Elsevier B.V.

This is an open access article under the CC BY-NC-ND license (<https://creativecommons.org/licenses/by-nc-nd/4.0>)

Peer-review under responsibility of SMAR 2024 Organizers

Keywords: Glulam; modal analysis; finite element updating; particle swarm optimization

* Corresponding author. Tel.: +34-942-201859.

E-mail address: sancibr@unican.es

1. Introduction

Glued laminated timber (Glulam) is a wood-derived product that combines the aesthetic qualities of sawn timber with improved mechanical properties, making it versatile for building structures such as auditoriums, sports facilities, footbridges and high-rise buildings (Fig. 1). However, laminated timber presents challenges compared to traditional construction materials. In fact, its non-homogeneous and anisotropic nature, influenced by humidity, makes structural modelling and analysis difficult. This makes non-destructive testing (NDT) techniques an important area of research. While there is an extensive literature on NDT for sawn timber, studies on such testing for glulam are scarce. The risk and responsibility associated with glulam structures is higher than that of sawn timber due to the larger dimensions of the structural elements.

NDT based on experimental modal analysis methods assumes that defects or damage alter stiffness, mass or damping characteristics, which can be assessed by measuring the dynamic response. Damage detection requires the evaluation of parameters such as eigenmodes and frequencies to distinguish between damaged and healthy components. However, it is necessary to consider the sensitivity of dynamic parameters to structural damage using a healthy model as a reference. Finite element (FE) model updating uses an intact theoretical model of the system as a reference, and experimental measurements are compared with the theoretical model to determine the changes caused by damage (Bru *et al.* 2016; Caicedo and Yun 2011).

FE model updating based on modal analysis is well established for materials with isotropic behaviour such as steel and other metals (Perera, Fang, and Huerta 2009; Perera, Marin, and Ruiz 2013). However, updating the theoretical model for complex materials such as glulam remains a challenge. Various approaches in the literature allow FE model updating for defect detection by modifying stiffness and mass matrices. Techniques such as Taguchi or Bayesian models, evolutionary algorithms and swarm theory have been used for this purpose (Kwon and Rong-Ming 2005; Mthembu *et al.* 2011; Lwin, Qu and Kendall 2014; Sindhya, Miettinen and Deb 2013). These methods use objective functions to minimise the difference between the real and theoretical models, aiming for a value close to zero that indicates a match between the models, and thus identify defects (Alkayem *et al.* 2018; Caicedo and Yun 2011).

This study presents a novel methodology using modal updating techniques specifically for glulam components. The primary objective is to evaluate the effectiveness of the method in detecting defects and variations in the modulus of elasticity (MOE) of the material. A number of glulam samples with minor defects such as concentrated knots, cracks and voids were meticulously analysed. The experimental results highlight the significant effect of knots and cracks on the MOE, confirming the effectiveness of the proposed method in detecting and characterising such defects. This research highlights the potential of modal updating techniques to improve defect detection and evaluation processes in glulam materials, thereby contributing to the advancement of structural integrity assessment methodologies for engineered wood products. This study's methodology for detecting defects in glulam components through modal updating techniques demonstrates the potential for improving the safety and reliability of glulam structures, thereby advancing the field of engineered wood products.

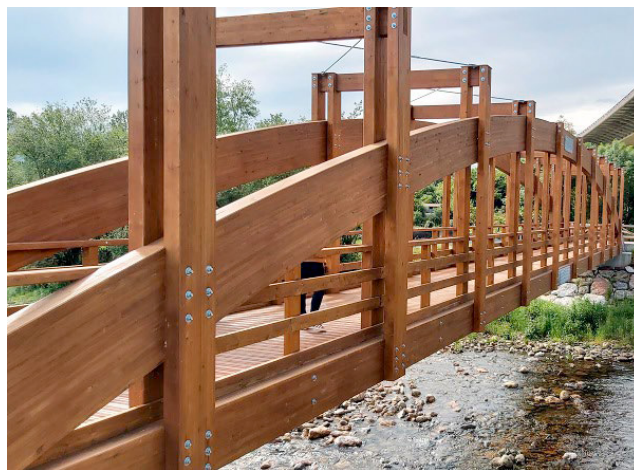


Fig. 1. Pedestrian footbridge made of Glulam.

Nomenclature

α_j	Damage parameter
β	Convergence threshold in PSO
ε	Error in natural frequencies
E_{st}	Static Young's Modulus
E_{dyn}	Dynamic Young's Modulus
\mathbf{E}	Vector of dynamic Young's Modulus in each substructure
\mathbf{K}	Stiffness matrix
\mathbf{M}	Mass matrix
μ	Eigenvalues
Φ	Eigenvector's matrix
ϕ	Mode shapes
ϕ_{ek}	Mode shapes obtained from modal analysis
ϕ_{tk}	Mode shapes obtained from numerical model
ω_{ek}	Natural frequencies obtained from modal analysis
ω_{tk}	Natural frequencies obtained from numerical model
MAC	Modal Assurance Criterion
V_p	Velocity of the particle
a	Weight of inertia
b_1, b_2	Acceleration coefficients
r_1, r_2	Random numbers
g_{best}	Best position of the group of particles
S_{max}	Size of the population
G_{max}	Maximum number of iterations

2. Description and characterization of Glulam samples

In this study, 12 duo-type glulam beams made of *Pinus Sylvestris* were tested. Each sample, graded GL24 and GL28 according to EN 14081:2000, consists of two lamellas glued with melamine urea formaldehyde (MUF) adhesive. This simple configuration was chosen to avoid introducing uncertainty. Visual inspection revealed no significant defects, though knots, cracks, and voids were noted in six samples (P01 to P06), which were evaluated using the Concentrated Knots Diameter Ratio (CKDR) method (Divos and Tanaka, 1997). The average length dimension of the samples was $L = 1.80$ m and the average width dimension was $D = 0.15$ m. The average height of each lamella was $h = 0.04$ m, and therefore the total height of each duo beam was $H = 0.08$ m. The average density of the *Pinus Sylvestris* samples is $\rho_{PS} = 491.9$ kg/m³ and $\rho_A = 472.8$ kg/m³ for the spruce.

The Static Modulus of Elasticity (E_{st}) was determined in the laboratory, providing accurate information on specimen health and potential defects affecting load-bearing capacity. However, due to impracticality for in-situ applications, it cannot be used as a Non-Destructive Testing (NDT) technique. In this study, E_{st} was used as a benchmark for the Modulus of Elasticity to assess the current condition of each sample.

3. Experimental procedure

To ensure repeatability and reproducibility a cantilever setup has been selected, providing easily controlled boundary conditions. To this aim, an adjustable metal support is constructed to securely clamp the specimens to a rigid wall. The test procedure carried out in this work is shown in Fig. 2 and is divided into the following 5 parts:

1. Experimental determination of the static modulus of elasticity (E_{st}). With the previously established boundary conditions, the beams are subjected to a known load P at their free end to obtain the deformation relationship and, consequently, determine the bending static modulus of elasticity of the material.
2. Theoretical modal analysis. The system is modelled using finite elements and the first four modes and natural frequencies are obtained, which are used as reference.

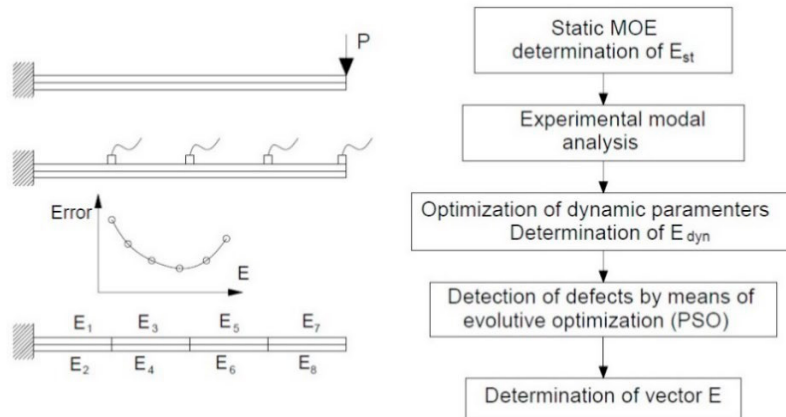


Fig. 2. Procedure for obtaining the stiffness distribution in specimens.

3. Experimental modal testing. The first four modes and natural frequencies are obtained through modal testing by exciting the system with an impact hammer and collecting the response with 4 accelerometers. Four mode shapes and four natural frequencies are recorded for each beam.
4. Obtain the dynamic modulus of elasticity by optimization. An error function is established to compare natural frequencies and theoretical-experimental modes. An optimization algorithm is used to find the minimum error using the dynamic modulus of elasticity (E_{dyn}) as the design variable. For this purpose, the beam is considered in a healthy state and with a homogeneous modulus of elasticity in all its dimensions.
5. Detection of damage through the variation of stiffness along the length of the beam. Each sample tested is modelled in finite elements by dividing it into 8 parts or substructures. Each part is assigned a variable representing the dynamic modulus of elasticity. The error between the experimental model and the theoretical one is reduced by optimization using a particle swarm optimization (PSO) algorithm.

In this way, the dynamic modulus of elasticity of each substructure is determined to fit the theoretical and experimental model. This variation in modulus provides information about the effect of defects in the material.

4. Experimental modal analysis

In this study, an Experimental Modal Analysis (EMA) was carried out for each specimen to determine the natural frequencies and modal shapes. The analysis considers that these parameters are influenced by factors such as modulus of elasticity, density, and geometry

Four capacitive accelerometers with a frequency range of 0 Hz to 1 kHz and a dynamic amplitude of 0 g to 10 g are placed along the major axes of the specimen. Double-sided adhesive tape is used to attach the accelerometers. A piezoelectric impulse force hammer (Kistler 9724A) with a force range of 0 N to 2000 N is used for system excitation. The signals from the accelerometers and the hammer are acquired by a measuring amplifier (HBM, QuantumX MX1601B) with a maximum sampling rate of 20 kHz per channel (see Fig. 3).



Fig. 3. Experimental modal analysis carried out in a duo-type glulam beam.

Modes and resonant frequencies are extracted using commercial experimental modal analysis software (ARTEMIS Modal v7.2). A roving hammer test is performed by hitting four locations near the accelerometer positions. The accelerometer and hammer signals are analyzed using the Rational Fraction Polynomial with complex Z mapping (RFP-z) and the Complex Mode Indication Function (CMIF) to isolate modes and resonant frequencies. An anti-aliasing filter is used to set the sampling frequency to 1200 Hz.

5. Model updating using modal analysis

In this study, modal properties are used to update the finite element model, focusing on the correlation between modal properties and mechanical properties of structural elements. The dynamic response of structures, defined by distributed stiffness, damping, and mass properties, relates modal properties to mass and stiffness matrices. Changes in these parameters allow Structural Damage Identification (SDI) through vibration measurement data. Ignoring damping effects, vibration dynamic parameters such as frequencies and mode shapes are derived by solving the eigenvalue problem:

$$(\mathbf{K} - \mu\mathbf{M})\Phi = 0 \quad (1)$$

Given that $\Phi \neq 0$, Eq. (1) yields a non-trivial solution, leading to the obtention of the natural frequencies ω_i by means of the following equation,

$$\det(\mathbf{K} - \mu\mathbf{M}) = 0 \quad (2)$$

By substituting these natural frequencies into Eq.(1) and solving the resulting system of equations mode shapes are determined. In this study, the first four natural frequencies and their corresponding mode shapes are utilized for mode updating. If the system is intact, the numerical model from Eq. (1) should match experimental results. However, damage alters stiffness values, requiring model updates. Structural damage is assumed to relate solely to stiffness variation, characterized by the damage parameter, α_j , which varies between 0 (undamaged) and 1 (total stiffness loss). This damage model is formulated using the following equation

$$K_{dj} = \sum_{j=1}^{ne} (1 - \alpha_j) K_{sj} \quad (3)$$

where K_{dj} is the stiffness of the j -th damaged substructure and K_{sj} is the stiffness of the same element without damage. In order to modelize the stiffness variation along the studied specimen, two numerical finite element models have been used in this work. Both models consist of 2359 quadratic tetrahedral elements. The first model (Model 1 in Fig. 4a) is homogeneous, which means that the stiffness is constant throughout its volume. The second model (Model 2 in Fig. 4b) is divided into 8 substructures (coloured green and white) so that each substructure can adopt a different stiffness value. In this way Model 2 can simulate stiffness losses and variations due to deterioration. After conducting a study to balance precision and efficiency, the division into 8 substructures was chosen. This division provides a detailed representation of the stiffness variations while maintaining computational efficiency.

Thus, the desing variables in model 2 are given by the following vector,

$$\mathbf{E} = [E_1 \ E_2 \ \dots \ E_8] \quad (4)$$

which E_i are the modulus of elasticity assigned to each substructure.

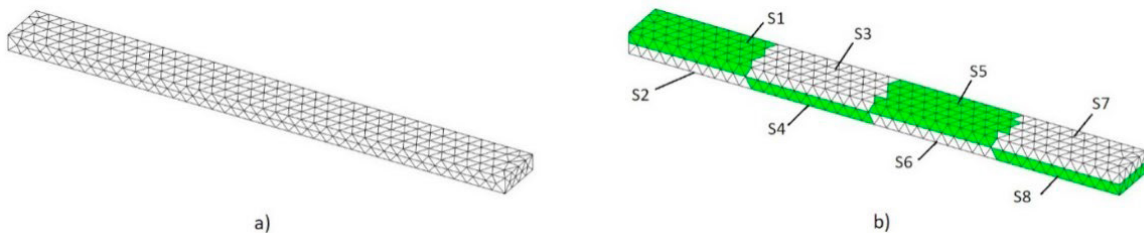


Fig. 4. (a) Homogeneous model and (b) non-homogenous model divided into eight substructures.

The comparison between the real and numerical models is done by comparing the natural frequencies and modes obtained from both models using the following objective function

$$F = \sum_{k=1}^{nf} \Delta\omega_k^2 + \sum_{k=1}^{nm} (1 - MAC_k) \tag{5}$$

where nf is the number of natural frequencies considered and nm is the number of modal shapes. For this study, both values are set equal to four.

The comparison of frequencies is carried out using Eq.(6), which quantifies the error between the theoretical natural frequencies, ω_{tk} , and the experimental ones, ω_{ek} .

$$\Delta\omega_k^2 = \left(\frac{\omega_{ek} - \omega_{tk}}{\omega_{tk}} \right)^2 \tag{6}$$

Meanwhile, the comparison of modes is achieved through the Modal Assurance Criterion (MAC) defined as:

$$MAC_i = \frac{(\Phi_{ti}^T \Phi_{ei})^2}{\|\Phi_{ti}\|^2 \|\Phi_{ei}\|^2} \tag{7}$$

here Φ_{ti} and Φ_{ei} represent the modal shapes obtained in the theoretical and experimental models, respectively. The MAC provides a measure of similarity between the modes obtained from both models (Allemang 2003).

6. Particle Swarm Optimization

The term Evolutionary Algorithms encompasses a range of algorithms designed to emulate natural phenomena in order to optimize a goal function (Alkayem et al. 2018; Greco et al. 2018). For this study, we use Particle Swarm Optimization (PSO), a method shown to be robust, effective, and reliable in numerous studies (Kang, Li, and Xu 2012). This section outlines the application of PSO, a variant of evolutionary algorithms, to model updating. PSO involves iterative refinement of a population, with a maximum size denoted as S_{max} . The velocity of particle p at iteration k , denoted v_p^k , is determined by the following equation:

$$v_p^{k+1} = av_p^k + b_1r_1(g_{best\ p} - E_p^k) + b_2r_2(g_{best} - E_p^k) \tag{8}$$

here, a is the weight of inertia, b_1 and b_2 are the acceleration coefficients, and r_1 and r_2 are random numbers generated uniformly between 0 and 1. The modulus of elasticity in each substructure at iteration k is denoted as E_p^k , which is updated to E_p^{k+1} in the next iteration (i.e., $k + 1$) by using the second equation:

$$E_p^{k+1} = E_p^k + v_p^{k+1} \tag{9}$$

Additionally, the best position of the particle j at iteration k is represented by $g_{best\ p}$, and the best position of the group up to iteration k is denoted as g_{best} . These parameters are kept constant throughout the optimization process, with values $a = 1.0$, and $b_1 = b_2 = 2.0$ as set in this work. The algorithm adjusts stiffness values in the finite element model to match experimental data, starting with a set of particles (vector E_p^k) stored in a matrix with dimensions corresponding to the substructures. A fixed population size of 100 particles is used. Two stopping criteria are employed: the process terminates after a maximum of 30 generations (G_{max}) or when the objective function value falls below $\beta < 1E-10$.

Table 1. Comparison of the modulus of elasticity between beams without defects and beams with defects.

MOE	Without defects			With defects		
	Static (MPa)	Dymanic (MPa)	Difference	Static (MPa)	Dymanic (MPa)	Difference
Mean value	10341.86	8916.67	15.98%	9520.93	8049.00	18.29%
Standard Deviation	360.94	1124.23		660.80	505.00	

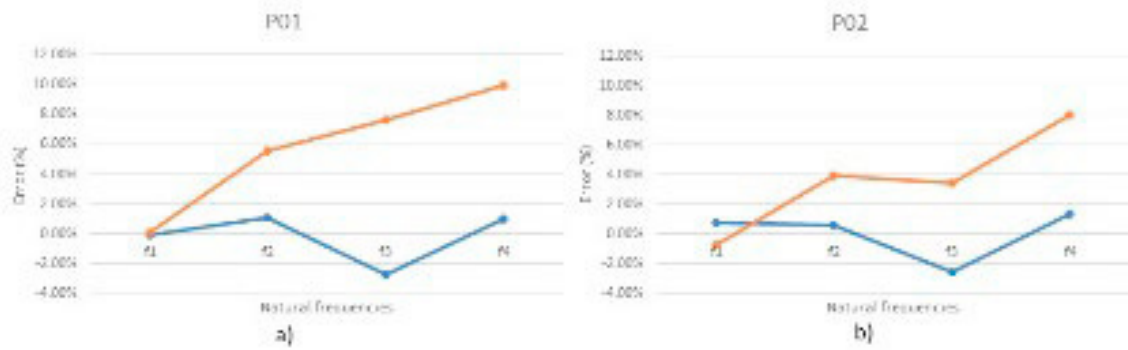


Fig. 5. Natural frequency errors obtained in homogeneous and non-homogeneous models.

7. Results

Table 1 shows the differences between E_{st} and E_{dyn} in specimens both with and without defects. It should be noted that E_{dyn} is smaller than E_{st} and this difference varies between 16% in healthy beams and 18% in beams with defects.

Once the optimization process has been carried out, errors between the experimentally obtained natural frequencies and the theoretical frequencies obtained through finite element updating have been analyzed. These errors are defined according to the following expression:

$$\varepsilon(\%) = \left| \frac{\omega_{ti} - \omega_{ei}}{\omega_{ei}} \right| 100; i = 1,2,3,4 \quad (10)$$

These defects are displayed for the samples with the highest number of defects (i.e., samples from P01 to P06). Figure 4 shows two examples of the results (specimens P01 and P02), which clearly demonstrate that homogeneous models do not correctly represent the dynamic behavior of glulam structures. In fact, there are variations in the natural frequencies on the order of 10%. However, the non-homogeneous model reduces these errors to less than 2% in most cases. Larger errors can occur, but it should be noted that in these cases, the subdivision into 8 substructures may not be sufficient to achieve the required accuracy. The modal comparison study follows a similar scheme. However, it is difficult to draw such clear conclusions with modal forms due to the difficulty of their representation.

Figure 5 shows the variation of the dynamic modulus of elasticity in the substructures of the same specimens with defects, obtained by updating the non-homogeneous finite element model. The comparison with the homogeneous finite element models can be observed in these figures. In the homogeneous models, the modulus obtained can be considered an average value, i.e., it does not account for local variations caused by the concentration of knots, cracks, or voids. However, these variations are accurately reflected in the non-homogeneous models. By observing the specimens, the authors correlated the loss of stiffness with the presence of knots and cracks. However, it was not possible to draw definitive conclusions about the influence of voids.

8. Conclusions

This paper presents a theoretical-experimental procedure for determining the dynamic modulus of elasticity in glulam structures. For this purpose, the static modulus of elasticity was first determined using conventional methods. This E_{st} serves in this work as a reference and comparison of the same modulus in the dynamic case. The E_{dyn} has been obtained experimentally by means of modal analysis, comparing these results with those obtained by means of finite elements. In a first stage, it was considered that the stiffness of the beam is uniform along its entire length, obtaining good results in the beams considered healthy. In a second stage, the optimization process is used to obtain the longitudinal variation of the stiffness in the samples. This variation has been obtained by optimization using a PSO algorithm. Duo-type samples have been used in this process with cantilever configuration in the structural analysis. The simplicity of these cases allows a reliable study since they present few sources of uncertainty. The results show that if the elements have no defects, a E_{dyn} can be obtained in a simple way. However, in the case where defects are present, it is necessary to resort to a more complex optimization considering several sections of different stiffness along the beam.

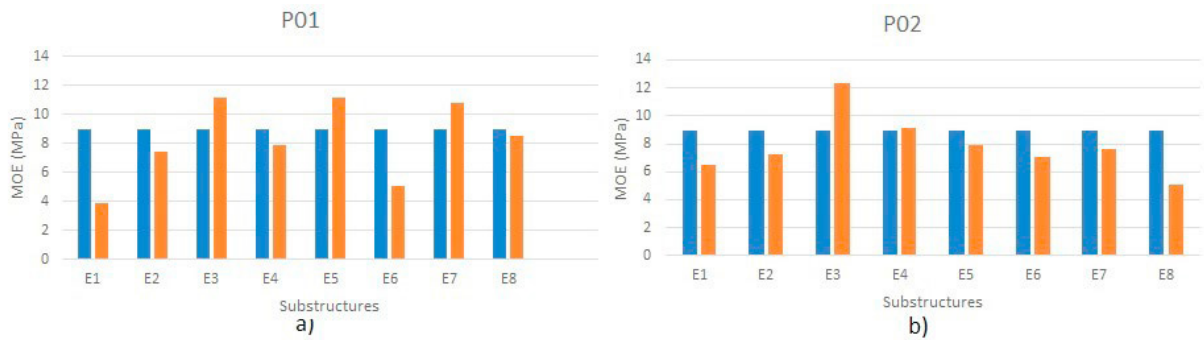


Fig. 6. Variations in dynamic modulus of elasticity among modeled substructures obtained through updating the non-homogeneous finite element model, along with its comparison to the homogeneous model.

One of the limitations of this work is the use of only 8 substructures. However, this number can be increased in future studies to improve the precision of the model. Expanding the number of substructures will allow for a more detailed representation of stiffness variations and could enhance the accuracy of the model updating process.

The PSO algorithm used in this work can be scaled to handle larger problems by increasing the population size or the number of generations, allowing for the optimization of more complex models with a greater number of substructures. Such scalability ensures that the PSO method can be effectively applied to a wide range of structural health monitoring and model updating tasks, regardless of the problem size.

Acknowledgements

This work was supported by the Spanish Ministry of Science and Innovation (Spain) under grant number TED2021-131522B-I00.

References

- Alkayem, Nizar Faisal, Maosen Cao, Yufeng Zhang, Mahmoud Bayat, and Zhongqing Su. 2018. "Structural Damage Detection Using Finite Element Model Updating with Evolutionary Algorithms: A Survey." *Neural Computing and Applications* 30(2):389–411. doi: 10.1007/s00521-017-3284-1.
- Allemang, Randall J. 2003. "The Modal Assurance Criterion - Twenty Years of Use and Abuse." *Sound and Vibration* 37(8):14–21.
- Bru, D., F. J. Baeza, F. B. Varona, J. García-Barba, and S. Ivorra. 2016. "Static and Dynamic Properties of Retrofitted Timber Beams Using Glass Fiber Reinforced Polymers." *Materials and Structures/Materiaux et Constructions* 49(1–2):181–91. doi: 10.1617/s11527-014-0487-0.
- Caicedo, Juan M., and Gun Jin Yun. 2011. "A Novel Evolutionary Algorithm for Identifying Multiple Alternative Solutions in Model Updating." *Structural Health Monitoring* 10(5):491–501. doi: 10.1177/1475921710381775.
- Divos, F., and Tanaka, T. 1997. "Lumber Strength Estimation by Multiple Regression". *Holzforschung* 51: 467-471.
- Greco, A., D. D'Urso, F. Cannizzaro, and A. Pluchino. 2018. "Damage Identification on Spatial Timoshenko Arches by Means of Genetic Algorithms." *Mechanical Systems and Signal Processing* 105:51–67. doi: 10.1016/j.ymsp.2017.11.040.
- Kang, Fei, Jun Jie Li, and Qing Xu. 2012. "Damage Detection Based on Improved Particle Swarm Optimization Using Vibration Data." *Applied Soft Computing Journal* 12(8):2329–35. doi: 10.1016/j.asoc.2012.03.050.
- Kwon, Kye Si, and Lin Rong-Ming. 2005. "Robust Finite Element Model Updating Using Taguchi Method." *Journal of Sound and Vibration* 280(1–2):77–99. doi: 10.1016/j.jsv.2003.12.013.
- Lwin, Khin, Rong Qu, and Graham Kendall. 2014. "A Learning-Guided Multi-Objective Evolutionary Algorithm for Constrained Portfolio Optimization." *Applied Soft Computing Journal* 24:757–72. doi: 10.1016/j.asoc.2014.08.026.
- Mthembu, Linda, Tshilidzi Marwala, Michael I. Friswell, and Sondipon Adhikari. 2011. "Model Selection in Finite Element Model Updating Using the Bayesian Evidence Statistic." *Mechanical Systems and Signal Processing* 25(7):2399–2412. doi: 10.1016/j.ymsp.2011.04.001.
- Perera, Ricardo, Sheng E. Fang, and C. Huerta. 2009. "Structural Crack Detection without Updated Baseline Model by Single and Multiobjective Optimization." *Mechanical Systems and Signal Processing* 23(3):752–68. doi: 10.1016/j.ymsp.2008.06.010.
- Perera, Ricardo, Roberto Marin, and Antonio Ruiz. 2013. "Static-Dynamic Multi-Scale Structural Damage Identification in a Multi-Objective Framework." *Journal of Sound and Vibration* 332(6):1484–1500. doi: 10.1016/j.jsv.2012.10.033.
- Sindhya, Karthik, Kaisa Miettinen, and Kalyanmoy Deb. 2013. "A Hybrid Framework for Evolutionary Multi-Objective Optimization." *IEEE Transactions on Evolutionary Computation* 17(4):495–511. doi: 10.1109/TEVC.2012.2204403.